11th World Congress on Computational Mechanics (WCCM XI)
5th European Conference on Computational Mechanics (ECCM V)
6th European Conference on Computational Fluid Dynamics (ECFD VI)
E. Oñate, J. Oliver and A. Huerta (Eds)

BAYESIAN UNCERTAINTY QUANTIFICATION AND PROPAGATION USING ADJOINT TECHNIQUES

COSTAS PAPADIMITRIOU, DIMITRIOS I. PAPADIMITRIOU

Department of Mechanical Engineering, University of Thessaly
Pedion Areos, Volos 38334, Greece.
e-mails: costasp@uth.gr, dpapadim@uth.gr, web page: http://www.mie.uth.gr/labs/sdl/

Key words: Bayesian Inference, Uncertainty Quantification, Parameter Estimation, Adjoint Methods

Abstract. This paper presents the Bayesian inference framework enhanced by analytical approximations for uncertainty quantification and propagation and parameter estimation. A Gaussian distribution is used to approximate the posterior distribution of the uncertain parameters. The most probable value of the parameters is obtained by minimizing the function defined as the minus of the logarithm of the posterior distribution and the covariance matrix of this posterior distribution is defined using asymptotic expansion as the inverse of the Hessian matrix of the aforementioned function, which is defined by the deviation of the computed quantities from corresponding experimental measurements. The gradient and the Hessian matrix of the objective function are computed using first and second-order adjoint approaches, respectively. The asymptotic approximation is also used to propagate the computed uncertainties of the model parameters to compute the uncertainty of the value of a quantity of interest. The presented approach is applied to the estimation of the uncertainties in the parameters of the Spalart-Allmaras turbulence model, based on experimental measurements that account for velocity and Reynolds stress distributions.

1 INTRODUCTION

The Bayesian inference framework for quantifying and propagating uncertainties in computational models of engineering systems has been adequately developed and widely used [1, 2, 3]. The framework aims at the selection among alternative plausible model structures to represent physical phenomenon and the unmodelled dynamics, estimation of the uncertainties in the parameters of these model structures, as well as propagation of uncertainties through the model to make robust predictions of output quantities of interest (QoI), consistent with available experimental measurements.

The Bayesian tools for identifying system and uncertainty models as well as performing robust prediction analyses are Laplace methods of asymptotic approximation and stochastic simulation algorithms [4, 5]. In analytical approximation, a Gaussian distribution is used to approximate the posterior distribution of the uncertain parameters. The most probable value of the parameters is obtained by minimizing the function defined as the minus of the logarithm of the posterior distribution and the covariance matrix of this posterior distribution is defined using asymptotic expansion as the inverse of the Hessian matrix of the aforementioned function, which is expressed as the deviation of the computed quantities from corrensponding experimental measurements. The Laplace asymptotic approximation is also used to propagate the computed uncertainties of the model parameters to compute the uncertainty in output QoI. The analytical approximations of the multi-dimensional probability integrals that arise in the propagation of uncertainties involve evaluations of appropriate objective function derivatives and Hessians.

Theoretical and computational issues involved in solving the optimization problems and computing the Hessian matrices are integrated in the Bayesian framework by developing direct differentiation and higher-order adjoint formulations [6, 7], including the differentiation of the turbulence model [8]. Analytical techniques have computational advantages since they require a moderate number of system re-analyses in comparison to the very large number of system re-analyses needed in the stochastic simulation algorithms. This computational efficiency, however, comes with the extra burden of developing the adjoint formulations and integrating them in system simulation software, a procedure that can be quite cumbersome for a number of computational models employed in engineering simulations.

A similar study for the estimation of turbulence model parameters using experimental data has been proposed in [11], based on the Bayesian approach. However, in this study, a stochastic optimization method was used, based on the Marcov Chain Monte Carlo theory, to find the posterior probability density function of the Spalart-Allmaras turbulence model parameters, so as the velocity and friction coefficient profiles confine to experimental data. The algorithm was applied to the flow over a flat plate.

Theoretical and computational developments are demonstrated by applying the proposed framework to the estimation of the parameters of the Spalart-Allmaras turbulence model [9] based on velocity and Reynolds stress measurements at a backward facing step flow [10].

2 BAYESIAN FRAMEWORK AND ASYMPTOTIC ANALYSIS

Assume that a CFD model (i.e. a RANS model described by the mean flow and turbulence model equations) is used to predict a quantity of interest (QoI) (such as the drag or lift of an airfoil/wing or the total pressure losses in a duct or a turbomachinery cascade) in a flow test case. Let $\underline{\theta}^p \in R^{N_{\theta^p}}$ represent the vector of parameters of the CFD model, such as the parameters involved in a turbulence model, whose values are to be estimated based on experimental data. Let $\underline{d} \in R^N$ be the vector of measured data of flow quantities available from experiments (such as velocities, Reynolds stresses, pressure coefficients, friction coefficients, etc) and $\underline{y}(\underline{\theta}^p) \in R^N$ be the vector of the values of the same quantities computed by the model for specific values of $\underline{\theta}^p$.

2.1 Uncertainty Quantification and Estimation

The objective is to quantify the uncertainty in the parameters $\underline{\theta}^p$ and model the missing (incomplete) information provided by the selected flow model given the experimental data, as well as to propagate these uncertainties through the flow model to predict the uncertainties in output QoI. Probability density functions (PDF) are used to quantify uncertainties and the calculus of probability is employed for handling and propagating uncertainties through the model in a consistent manner. To model the incomplete information due to the selection of a particular flow model, a probabilistic model is built to characterize the deviation between the experimental and the model predicted values. For this, the measured data and the corresponding model predictions satisfy the prediction error equation

$$\underline{d} = \underline{y}(\underline{\theta}^p) + \underline{e} \tag{1}$$

where $\underline{e}$ is the prediction error due to the measurement, computational and modeling uncertainties. Assuming that the prediction error is characterized by a zero-mean and a covariance Σ, the principle of maximum entropy is invoked to model the prediction error by a Gaussian vector. It is assumed that the structure of the covariance matrix depends on a parameter set $\underline{\theta}^e$, ($\Sigma \equiv \Sigma(\underline{\theta}^e) \in R^{N \times N}$). The parameters $\underline{\theta}^e = (\sigma, \lambda)$ are estimated jointly with $\underline{\theta}^p$, based on the experimental measurements.

Following a Bayesian formulation [3], the posterior PDF of the combined parameter set $\underline{\theta} = (\underline{\theta}^p, \underline{\theta}^e)$ given the measured data $\underline{d}$, is given by

$$p(\underline{\theta}|\underline{d}) = \frac{p(\underline{d}|\underline{\theta})\pi(\underline{\theta})}{p(\underline{d})} \tag{2}$$

where $p(\underline{d}|\underline{\theta})$ is the *likelihood* of observing the data $\underline{d}$ from the model for given values of the parameters $\underline{\theta}$, $\pi(\underline{\theta})$ is the *prior* probability of the parameters $\underline{\theta}$, and $p(\underline{d})$ is the *evidence* of the model class given by

$$p(\underline{d}) = \int p(\underline{d}|\underline{\theta})\pi(\underline{\theta})d\underline{\theta} \tag{3}$$

so that the posterior PDF integrates to one. Using the Gaussian model for the prediction error $\underline{e}$, the likelihood function is given by

$$p(\underline{d}|\underline{\theta}) = \frac{1}{(2\pi)^{\frac{N}{2}} det\Sigma^{\frac{1}{2}}} exp\left[-\frac{1}{2}J(\underline{\theta};\underline{d})\right] \tag{4}$$

where

$$J(\underline{\theta};\underline{d}) = [\underline{d} - \underline{y}(\underline{\theta}^p)]^T \Sigma(\underline{\theta}^e)^{-1} [\underline{d} - \underline{y}(\underline{\theta}^p)] \tag{5}$$

expresses the deviation between the measured and model predicted quantities.

Using a well-established analytical approximation, valid for large number of experimental data, the posterior distribution of the model parameters can be approximated by a multi-variable Gaussian distribution

$$p(\underline{\theta}|\underline{d}) \sim p_a(\underline{\theta}|\underline{d}) = \frac{1}{(2\pi)^{\frac{N_\theta}{2}} det H^{-\frac{1}{2}}} exp\left[-\frac{1}{2}\left(\underline{\theta} - \hat{\underline{\theta}}\right)^T H(\hat{\underline{\theta}})\left(\underline{\theta} - \hat{\underline{\theta}}\right)\right] \tag{6}$$

centered at the most probable value $\hat{\underline{\theta}}$ of the posterior distribution function or equivalently the minimum of the function

$$L(\underline{\theta}) = -log(p(\underline{d}|\underline{\theta})\pi(\underline{\theta})) \tag{7}$$

given by

$$\hat{\underline{\theta}} = \arg\min_{\underline{\theta}} [L(\underline{\theta})] \tag{8}$$

and with covariance $C(\hat{\underline{\theta}})$ equal to the inverse of the Hessian $H(\hat{\underline{\theta}})$ of the function $L(\underline{\theta})$ estimated at the most probable value $\hat{\underline{\theta}}$. The uncertainty in $\underline{\theta}$ can thus be fully described asymptotically by solving an optimization problem for finding the most probable value $\hat{\underline{\theta}}$ that minimizes the function $L(\underline{\theta})$, and also evaluating the Hessian of the function $L(\underline{\theta})$ at a single point $\hat{\underline{\theta}}$. Herein it is assumed that only one global optimum exists with probability volume that dominates the ones corresponding to multiple local optima. The analysis can be extended to account for more than one global/local optima with comparable probability volumes contributing to the posterior PDF [3].

An asymptotic estimate of the evidence of the model class based on Laplace approximation of the integral (3) is given by [1, 2, 12]).

$$p(\underline{d}) = \frac{(2\pi)^{\frac{N_\theta}{2}}}{[det H(\hat{\underline{\theta}})]^{1/2}} exp[-L(\hat{\underline{\theta}})] \tag{9}$$

This estimate can be used for comparing competing models.

2.2 Uncertainty Propagation

Let $g(\underline{\theta}, \eta)$ be an output QoI that is evaluated by

$$g(\underline{\theta}, \eta) = g_m(\underline{\theta}) + \eta \tag{10}$$

where $g_m(\underline{\theta})$ is the prediction of the QoI from the flow model and η is the prediction error accounting for the model error. As in the case of measured QoI, the model error can be assumed to be Gaussian with zero mean and variance σ_η^2. The uncertainty in the output QoI can be obtained by propagating the uncertainty in the parameter set $\underline{\theta}$ through the flow model and taking into account the model error uncertainty.

The uncertainty is next described by the mean and the standard deviation of the quantity $g(\underline{\theta}, \eta)$. Using eq. (10), the mean is readily computed as

$$E[g(\underline{\theta}, \eta)] = E[g_m(\underline{\theta})] \tag{11}$$

The standard deviation is estimated through the second moment which, taking into account that $g_m(\underline{\theta})$ and η are independent variables, one readily derives from eq. (10) that

$$E[g^2(\underline{\theta}, \eta)] = E[g_m^2(\underline{\theta})] + \sigma_\eta^2 \tag{12}$$

The variance of the QoI is finally obtained from

$$Var[g(\underline{\theta}, \eta)] = Var[g_m(\underline{\theta})] + \sigma_\eta^2 \tag{13}$$

where

$$Var[g_m(\underline{\theta})] = E[g_m^2(\underline{\theta})] - \{E[g_m(\underline{\theta})]\}^2 \tag{14}$$

The posterior mean value of $g_m(\underline{\theta})$ is given as

$$E[g_m(\underline{\theta})] = \int g_m(\underline{\theta}) p(\underline{\theta}|\underline{d}) d\underline{\theta} \tag{15}$$

and the posterior second moment is

$$E[g_m^2(\underline{\theta})] = \int g_m^2(\underline{\theta}) p(\underline{\theta}|\underline{d}) d\underline{\theta} \tag{16}$$

Substituting the expression of the posterior PDF in eq. (15) yields

$$E[g_m(\underline{\theta})] = \frac{\int g_m(\underline{\theta}) p(\underline{d}|\underline{\theta}) \pi(\underline{\theta}) d\underline{\theta}}{\int p(\underline{d}|\underline{\theta}) \pi(\underline{\theta}) d\underline{\theta}} \tag{17}$$

The Laplace asympotic estimate for the denominator is given in eq. (9). Applying a similar asymptotic estimate for the numerator, one readily obtains the following asymptotic estimate for the mean value of $g_m(\underline{\theta})$

$$E[g_m(\underline{\theta})] = exp[L(\hat{\underline{\theta}}) - L_g(\hat{\underline{\theta}}_g)] \frac{[detH(\hat{\underline{\theta}})]^{1/2}}{[detH_g(\hat{\underline{\theta}}_g)]^{1/2}} \tag{18}$$

where

$$\hat{\underline{\theta}}_g = \arg\min_{\underline{\theta}} [L_g(\underline{\theta})] \tag{19}$$

the function $L_g(\underline{\theta})$ is given by

$$L_g(\underline{\theta}) = -log(g_m(\underline{\theta})p(\underline{d}|\underline{\theta})\pi(\underline{\theta})) = -log(g_m(\underline{\theta})) + L(\underline{\theta}) \tag{20}$$

and $H_g(\hat{\underline{\theta}}_g)$ is the Hessian matrix of the function $L_g(\underline{\theta})$ evaluated at $\hat{\underline{\theta}}_g$.

Following the same procedure for the integral in eq. (16) that gives the second moment, it can be readily shown that

$$E[g_m^2(\underline{\theta})] = exp[L(\hat{\underline{\theta}}) - L_{g^2}(\hat{\underline{\theta}}_{g^2})] \frac{[detH(\hat{\underline{\theta}})]^{1/2}}{[detH_{g^2}(\hat{\underline{\theta}}_{g^2})]^{1/2}} \tag{21}$$

where

$$\hat{\underline{\theta}}_{g^2} = \arg\min_{\underline{\theta}} [L_{g^2}(\underline{\theta})] \tag{22}$$

with $L_{g^2}(\underline{\theta})$ given by

$$L_{g^2}(\underline{\theta}) = -log(g_m^2(\underline{\theta})p(\underline{d}|\underline{\theta})\pi(\underline{\theta})) = -log(g_m^2(\underline{\theta})) + L(\underline{\theta}) \tag{23}$$

and $H_{g^2}(\hat{\underline{\theta}}_{g^2})$ is the Hessian of $L_{g^2}(\underline{\theta})$ evaluated at $\hat{\underline{\theta}}_{g^2}$.

The mean and the standard deviation derived based on the asymptotic approximations 18 and 21 give robust prediction of the output QoI that take into account the uncertainty in the turbulence model parameters and prediction error model parameters. The computation of the mean value and variance of any output QoI $g(\underline{\theta}, \eta)$ requires the solution of two additional optimization problems (19) and (22) and the computation of a Hessian matrix at each optimal solution. To considerably accelerate convergence to the optimal solutions of the aforementioned optimization problems, the most probable solution $\hat{\underline{\theta}}$ in (8) can be used as starting point in both problems. It is evident that the first and second-order adjoint methods for turbulence models in CFD are useful techniques for considerably reducing the computational effort associated with the three optimization problems (8), (19) and (22), as well as computing the Hessian of the three objective functions involved.

3 COMPUTATION OF FIRST AND SECOND-ORDER SENSITIVITIES

The objective function to be minimized is given in eq. (7) which can be expressed in tensor form as

$$L \;=\; \frac{1}{2}(y_k - d_k)\Sigma_{kl}^{-1}(y_l - d_l) + \frac{1}{2}log(det\Sigma) + \frac{N}{2}log(2\pi) + L_\pi \tag{24}$$

where the summation is implied for indices k and l with $1 < k, l < N$, the notation $\Sigma^{-1}_{kl} \equiv [\Sigma^{-1}]_{kl}$ is used, and y_k (and d_k) stand for the values of computed (and experimental) axial velocities (u_1) or Reynolds shear stresses $\mu_t(\frac{\partial u_1}{\partial x_2} + \frac{\partial u_2}{\partial x_1})$. The computed quantities y_k are interpolated at the locations where the experimental values are provided. The last term L_π is defined as

$$L_\pi \equiv L_\pi(\underline{\theta}) = -log(\pi(\underline{\theta})) \tag{25}$$

The differentiation of eq. (24) with respect to θ_i yields

$$\frac{dL}{d\theta_i} = (y_k - d_k)\Sigma^{-1}_{kl}\frac{dy_l}{d\theta_i} + \frac{1}{2}(y_k - d_k)\frac{d\Sigma^{-1}_{kl}}{d\theta_i}(y_l - d_l) + \frac{1}{2}\frac{dlog(det\Sigma)}{d\theta_i} + \frac{\partial L_\pi}{\partial\theta_i} \tag{26}$$

without summation for the index i. The sensitivities of L with respect to θ^p_i are given by

$$\frac{dL}{d\theta^p_i} = (y_k - d_k)\Sigma^{-1}_{kl}\frac{\partial y_l}{\partial U_m}\frac{dU_m}{d\theta^p_i} + \frac{\partial L_\pi}{\partial\theta^p_i} \tag{27}$$

where $U_m = 0$ stand for the discretized mean flow and turbulence model variables ($1 < m < N_g$, where N_g is the number of grid nodes multiplied by 5 (the number of mean flow and turbulence model equations). $\frac{dL}{d\theta^p_i}$ are computed directly by solving the adjoint equations

$$(y_k - d_k)\Sigma^{-1}_{kl}\frac{\partial y_l}{\partial U_m} + \Psi_n\frac{\partial R_n}{\partial U_m} = 0 \tag{28}$$

with a cost almost equal to the cost for solving the flow equations, using the expression

$$\frac{d\tilde{L}}{d\theta^p_i} = \Psi_n\frac{\partial R_n}{\partial\theta^p_i} + \frac{\partial L_\pi}{\partial\theta^p_i}$$

On the other hand, the sensitivities of L with respect to θ^e_i are computed analytically by the expression

$$\frac{dL}{d\theta^e_i} = \frac{1}{2}(y_k - d_k)\frac{d\Sigma^{-1}_{kl}}{d\theta^e_i}(y_l - d_l) + \frac{1}{2}\frac{dlog(det\Sigma)}{d\theta^e_i} + \frac{\partial L_\pi}{\partial\theta^e_i} \tag{29}$$

Finally, the sensitivities of the objective function $L_g(\underline{\theta})$ and $L_{g^2}(\underline{\theta})$ with respect to θ^p_i can be computed analytically following a similar adjoint formulation that involves the output QoI $L_g(\underline{\theta})$ and $L_{g^2}(\underline{\theta})$ appearing in (19) and (22), respectively.

The second-order sensitivities of L with respect to θ^p_i are computed using the combination of direct differentiation with the adjoint approach, from the expression

$$\begin{aligned}\frac{d^2\bar{L}}{d\theta^p_i d\theta^p_j} &= \left(\Psi_q\frac{\partial^2 R_q}{\partial U_m\partial U_n} + (y_k - d_k)\Sigma^{-1}_{kl}\frac{\partial^2 y_l}{\partial U_m\partial U_n} + \Sigma^{-1}_{kl}\frac{\partial y_k}{\partial U_n}\frac{\partial y_l}{\partial U_m}\right)\frac{dU_m}{d\theta^p_i}\frac{dU_n}{d\theta^p_j} \\ &+ \Psi_q\left(\frac{\partial^2 R_q}{\partial\theta^p_i\partial U_m}\frac{dU_m}{d\theta^p_j} + \frac{\partial^2 R_q}{\partial U_m\partial\theta^p_j}\frac{dU_m}{d\theta^p_i}\right) + \Psi_q\frac{\partial^2 R_q}{\partial\theta^p_i\partial\theta^p_j} + \frac{\partial^2 L_\pi}{\partial\theta^p_i\partial\theta^p_j}\end{aligned} \tag{30}$$

where Ψ_q is the solution of eq. (28) and $\frac{dU_m}{d\theta_i^p}$ using the direct differentiation of the flow equations. The second-order derivatives of L with respect to θ^e are computed analytically by differentiating eq. (29), yielding

$$\frac{d^2L}{d\theta_i^e d\theta_j^e} = \frac{1}{2}(y_k - d_k)\frac{d^2\Sigma_{kl}^{-1}}{d\theta_i^e d\theta_j^e}(y_l - d_l) + \frac{1}{2}\frac{d^2 log(det\Sigma)}{d\theta_i^e d\theta_j^e} + \frac{\partial^2 L_\pi}{\partial\theta_i^e \partial\theta_j^e} \tag{31}$$

and the mixed derivatives of L with respect to θ_i^p and θ_j^e are derived by differentiating eq. (27) with respect to θ^e

$$\frac{d^2L}{d\theta_i^p d\theta_j^e} = (y_k - d_k)\frac{d\Sigma_{kl}^{-1}}{d\theta_j^e}\frac{\partial y_l}{\partial U_m}\frac{dU_m}{d\theta_i^p} \tag{32}$$

4 APPLICATIONS

The proposed algorithm is applied to the quantification of the uncertainties of the eight parameters of the Spalart-Allmaras turbulence model and the parameters of the prediction error model in the flow through a 2D backward facing step configuration [10]. The flow domain is shown in Fig. 1, used in $http://turbmodels.larc.nasa.gov/backstep\_val.html$. The flow through the 2D backward facing step is a well known test case configuration for which several experiments have been conducted. The turbulent boundary layer encounters a sudden back step, causing flow separation. The flow then reattaches and recovers downstream of the step. The Reynolds number based on step height is equal to 36000 and the inlet Mach number is equal to 0.128. The step height is equal to $1m$, while the distance between the top and bottom walls is equal to $9m$ (after the step).

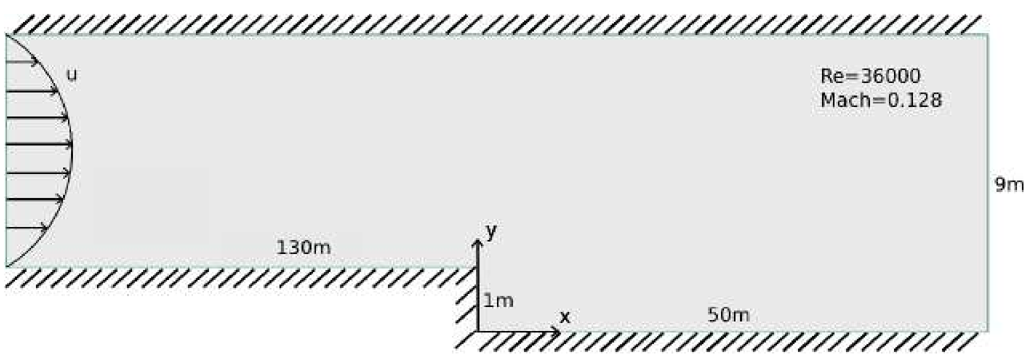

Figure 1: Schematic view of the backward facing step case.

The experimental data used for the quantification of uncertainties are the axial velocity and Reynolds shear stress profiles at five longitudinal positions. The experimental data and the measured positions within the flow domain can be found in [10] and in the aforementioned site of NASA. The first position is $4m$ before the step and the other four ones are $1m$, $4m$, $6m$ and $10m$ after the step. A computational grid with 4992 quadrilateral elements, obtained from the same site, is used to carry out the simulations.

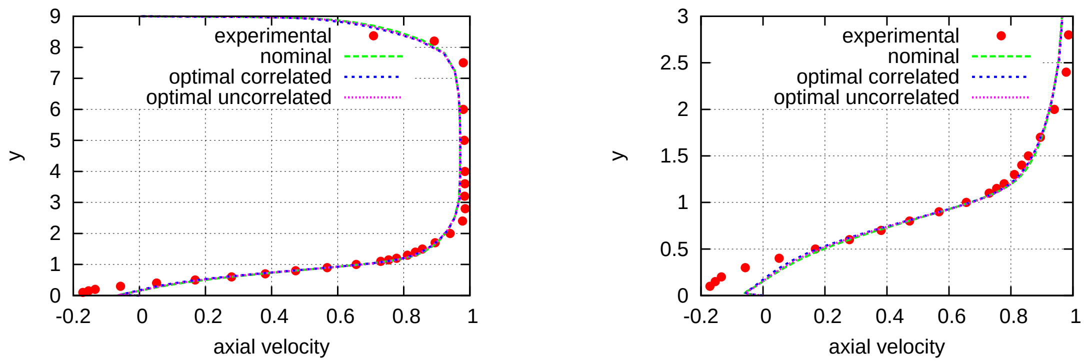

Figure 2: Comparison of the optimal velocity distributions at location $4m$ after the step based on the optimal values of the model parameters for the correlated and uncorrelated case with the experimental distributions based on measurements. The right figure is a close-up view at the separation region where $y < 3$.

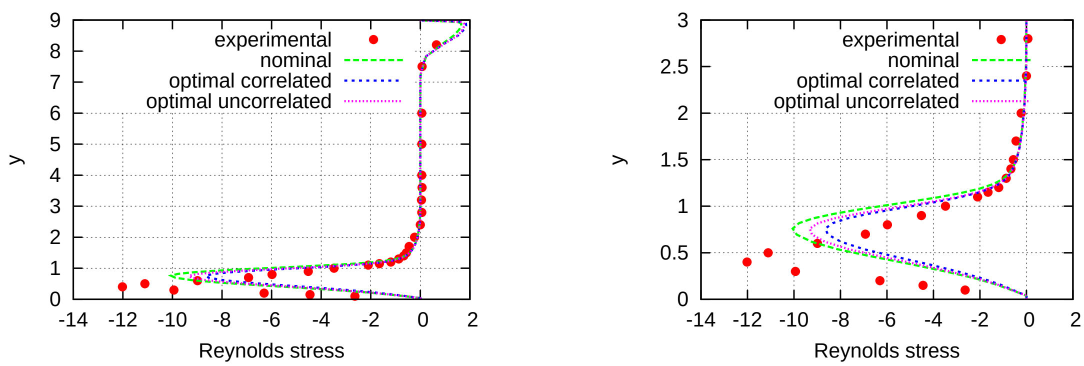

Figure 3: Comparison of the optimal Reynolds stress distributions at location $4m$ after the step based on the optimal values of the model parameters for the correlated and uncorrelated case with the experimental distributions based on measurements. The right figure is a close-up view at the separation region where $y < 3$.

	κ	c_{v_1}	c_{v_2}	c_{b_1}	c_{b_2}	c_{w_2}
nominal value	0.410	7.100	5.000	0.1355	0.622	0.300
optimal value (correlated)	0.471	6.817	4.950	0.1039	0.639	0.314
optimal value (uncorrelated)	0.456	7.591	4.749	0.1102	0.637	0.335
COV (prior)	0.200	0.200	0.200	0.2000	0.200	0.200
COV (posterior, correlated)	0.109	0.126	0.195	0.0712	0.193	0.172
COV (posterior, uncorrelated)	0.087	0.097	0.200	0.0535	0.194	0.175

Table 1: Initial and optimal parameter values and coefficients of variation (COV) using the adjoint approach for the correlated and the uncorrelated case (first six parameters).

Two models are considered for the correlation of the computational errors. The first one is based on a spatial correlation length model where the computational errors are

	c_{w_3}	σ_{SA}	σ_{VEL}	λ_{VEL}	σ_{RS}	λ_{RS}
nominal value	2.000	0.667	0.035	0.800	1.000	0.200
optimal value (correlated)	1.976	0.770	0.036	0.819	1.156	0.248
optimal value (uncorrelated)	2.074	0.915	0.039	-	1.436	-
COV (prior)	0.200	0.200	-	-	-	-
COV (posterior, correlated)	0.200	0.148	0.145	0.386	0.073	0.189
COV (posterior, uncorrelated)	0.178	0.120	0.062	-	0.064	-

Table 2: Initial and optimal parameter values and coefficients of variation (COV) using the adjoint approach for the correlated and the uncorrelated case (rest six parameters).

assumed correlated according to their spatial distance and the second one disregards any spatial correlation. Results demonstrate that the measurements provide information for estimating three to five among the eight parameters of the turbulence model, while the rest of the parameters are insensitive to the information contained in the data. Model validation using the experimental measurements suggest that the Spalart-Allmaras model is not adequate enough to accurately predict velocities and Reynolds stresses in certain region in the flow domain where flow separation phenomena are dominant. This is manifested by the high prediction error uncertainty in these regions in relation to the prediction uncertainty arising from the turbulence model parameter uncertainty. Among the two prediction error model classes considered, the spatially correlated one is clearly promoted as the best model by the Bayesian model selection methodology.

In Tables 1 and 2, the initial and optimal values of the parameters using the proposed method are shown for the correlated and uncorrelated prediction error model, respectively. The coefficients of variation (COV) of the marginal distribution of each model parameter, defined as the ratio of the standard deviation over the mean (optimal) value of each model parameter, are also reported in these tables. For the Gaussian posterior distribution, the standard deviation of the i-th parameter is the square root of the i diagonal element of the covariance matrix. The experimental data are informative for a particular turbulence model parameter if the COV of the marginal posterior PDF of this parameter is reduced compared to the COV of the prior PDF. It can be seen from the results in Tables 1 and 2 that the most well-informed parameters are κ, c_{v_1} and c_{b_1}. The uncertainty in c_{w_2} and σ_{SA} has a smaller reduction in relation to the prior uncertainty. The rest of the parameters c_{v_2}, c_{b_2} and c_{w_3} retained the COV at approximately the level given by the prior Gaussian distribution, indicating that the data do not provide valuable information for identifying the values and uncertainty in these parameters.

The Bayesian asymptotic analysis is then used to propagate uncertainties to the total pressure losses, computed as the difference in average total pressure p_t between the inlet and the outlet of the flow domain $A_I^{-1}\int_{S_I} p_t dS - A_O^{-1}\int_{S_O} p_t dS$ where A_I and A_O are the inlet and outlet areas, respectively. Accounting for the uncertainty in the turbulence model parameters, the predicted mean value is equal to $2.752E-3$ and the standard deviation is equal to $1.250E-4$, which corresponds to coefficient of variation of 4.5%, for the correlated model error case. In the case of the uncorrelated error model the mean value of the total pressure losses is equal to $2.277E-3$ and the standard deviation is equal to $1.592E-3$, which corresponds to coefficient of variation of 6.7%. It seems that the uncertainty propagation results depend on the prediction error model used. Finally, it should be noted that the uncertainties reported ignore uncertainties due to prediction error model that arise from the model inadequacy. In contrast to the velocity and Reynolds stresses, there is no information to compute such prediction error uncertainties since the experimental values of the pressure losses are not available. As it was derived in the theory (see equation (14)), the prediction error model uncertainties will be insignificant for standard deviations σ_η much smaller than the standard deviations $STD(g_m(\underline{\theta}))$ derived from the uncertainties in the model parameters. However, for standard deviations σ_η much larger than the ones derived from the uncertainties in the model parameters, the prediction error uncertainties will dominate the overall uncertainty in the pressure losses.

5 CONCLUSIONS

A Bayesian framework was presented for uncertainty quantification and propagation combining analytical asymptotic approximations with higher-order adjoint methods to estimate the posterior PDF of the flow and prediction error model parameters, select the best model among competitive prediction error models and propagate uncertainties through CFD model simulations for making robust predictions of important output QoI.

The framework was applied for the estimation of the parameters of the Spalart-Allmaras turbulence model based on velocity and Reynolds stress measurements at a backward facing step flow. Results demonstrated that the measurements provide information for estimating three to five among the eight parameters of the turbulence model, while the rest of the parameters were insensitive to the information contained in the data.

ACKNOWLEDGMENTS

The research project is implemented within the framework of the Action “Supporting Postdoctoral Researchers” of the Operational Program “Education and Lifelong Learning” (Actions Beneficiary: General Secretariat for Research and Technology), and is co-financed by the European Social Fund (ESF) and the Greek State.

REFERENCES

[1] K.V. Yuen, Bayesian methods for structural dynamics and civil engineering, John Wiley & Sons, 2010.

[2] C. Papadimitriou, L.S. Katafygiotis, A Bayesian methodology for structural integrity and reliability assessment, International Journal of Advanced Manufacturing Systems, 4(1) (2001) 93-100.

[3] J.L. Beck, L.S. Katafygiotis, Updating models and their uncertainties. I: Bayesian statistical framework, Journal of Engineering Mechanics, ASCE., 124(4) (1998) 455-461.

[4] P. Angelikopoulos, C. Papadimitriou, P. Koumoutsakos, Bayesian uncertainty quantification and propagation in molecular dynamics simulations: a high performance computing framework, The Journal of Chemical Physics, 137(14) (2012) 103-144.

[5] C. Papadimitriou, J.L. Beck, L.S. Katafygiotis, Updating robust reliability using structural test data, Probabilistic Engineering Mechanics, 16(2) (2001) 103-113.

[6] L.L. Sherman, A.C. Taylor III, L.L. Green, P.A. Newman, J.W. Hou, V.M. Korivi, First- and second-order aerodynamic sensitivity derivatives via automatic differentiation with incremental iterative methods, Journal of Computational Physics, 129 (1996) 307-331.

[7] D.I. Papadimitriou, K.C. Giannakoglou, Aerodynamic shape optimization using first and second order adjoint and direct approaches, Archives of Computational Methods in Engineering, (State of the Art Reviews), 15(4) (2008) 447-488.

[8] A.S. Zymaris, D.I. Papadimitriou, K.C. Giannakoglou, C. Othmer, Continuous adjoint approach to the Spalart-Allmaras turbulence model for incompressible flows, Computers and Fluids, 38 (2009) 1528-1538.

[9] P. Spalart, S. Allmaras, A one-equation turbulence model for aerodynamic flows, AIAA paper, 92-0439, 1992.

[10] D.M. Driver, H.L. Seegmiller, Features of reattaching turbulent shear layer in divergent channel flow, AIAA Journal, 23(2) (1985), 163-171.

[11] S.H. Cheung, T.A. Oliver, E.E. Prudencio, S. Prudhomme, R.D. Moser, Bayesian uncertainty analysis with applications to turbulence modeling, Reliability Engineering and System Safety, 96 (2011) 1137-1149.

[12] S.H. Cheung, J.L. Beck, Calculation of posterior probabilities for Bayesian model class assessment and averaging from posterior samples based on dynamic system data, Journal of Computer-aided Civil and Infrastructure Engineering, 25(5) (2010) 304-321.

[13] C. Papadimitriou, G. Lombaert, The effect of prediction error correlation on optimal sensor placement in structural dynamics, Mechanical Systems and Signal Processing, 28 (2012) 105-127.